4 Finite elements

We now tackle the convergence analysis of the discrete version of problem (27), magnetostatics:

$$\mathbf{D}\mathbf{b} = 0, \mathbf{h} = \boldsymbol{\nu}\mathbf{b}, \mathbf{R}^t\mathbf{h} = \mathbf{j}. \tag{39}$$

A preliminary comment on what that means is in order.

A few notational points. The mesh is denoted m, the dual mesh is $\widetilde{\mathrm{m}}$, and we shall subscript by m, when necessary, all mesh-related entities. For instance, the largest diameter of all p-cells, $p \geq 1$, primal and dual, will be denoted γ_{m} (with a mild abuse, since it also depends on the metric of the dual mesh), and called the "grain" of the pair of meshes. The computed solution $\{\mathbf{b}, \mathbf{h}\}$ will be $\{\mathbf{b}_{\mathrm{m}}, \mathbf{h}_{\mathrm{m}}\}$ when we wish to stress its dependence on the mesh-pair. And so on.

A first statement of our purpose is "study $\{\mathbf{b}_{\mathrm{m}}, \mathbf{h}_{\mathrm{m}}\}$ when γ_{m} tends to 0". Alas, this lacks definiteness, because how the *shapes* of the cells change in the process does matter a lot. In the case of triangular 2D meshes, for instance, there are well-known counter-examples [4] showing that, if one tolerates too much "flattening" of the triangles as the grain tends to 0, convergence may fail to occur. Hence the following definition: A family $\mathcal{M}$ of (pairs of interlocked) meshes is *uniform* if there is a *finite* catalogue of "model cells" such that any cell in any m or $\widetilde{\mathrm{m}}$ of the family is similar to one of them. The notation "$\mathrm{m} \to 0$" will then refer to a sequence of meshes, all belonging to some definite uniform family, and such that their γ_{m}s tend to zero. Now we redefine our objective: Show that the error, whatever one means by that, incurred by taking $\{\mathbf{b}_{\mathrm{m}}, \mathbf{h}_{\mathrm{m}}\}$ as a substitute for the real field $\{b, h\}$, tends to zero when $\mathrm{m} \to 0$.

The practical implications of achieving this are well known. If, for a given m, the computed solution $\{\mathbf{b}_{\mathrm{m}}, \mathbf{h}_{\mathrm{m}}\}$ is not deemed satisfactory, one must *refine* the mesh and redo the computation, again and again. If the refinement rule guarantees that all meshes such a process can generate belong to some definite uniform family, then the convergence result means "you may get as good an approximation as you wish by refining this way", a state of affairs we are more or less happy to live with.

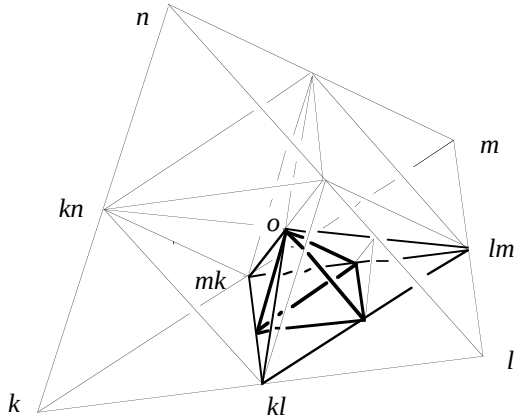

Figure 30. Subdivision rule for a tetrahedron $\mathrm{T} = \{k, l, m, n\}$. (Mid-edges are denoted kl, lm, etc., and o is the barycenter.) A first halving of edges generates four small tetrahedra and a core octahedron, which itself can be divided into eight "octants" such as $\mathrm{O} = \{o, kl, lm, mk\}$, of at most four different shapes. Now, octants like O should be subdivided as follows: divide the facet in front of o into four triangles, and join to o, hence a tetrahedron similar to T, and three peripheral tetrahedra. These, in turn, are halved, as shown for the one hanging from edge $\{o, lm\}$. Its two parts are similar to O and to the neighbor octant $\{o, kn, kl, mk\}$ respectively.

Fortunately, such refinement rules do exist (this is an active area of research [8, 9, 28, 66]). Given a pair of coarse meshes to start with, there are ways to subdivide the cells so as to keep bounded the number of different cell-shapes that appear in the process, hence a potential

infinity of refined meshes, which do constitute a uniform family. (A refinement process for tetrahedra is illustrated by Fig. 30. As one can see, at most five different shapes can occur, for each tetrahedral shape present in the original coarse mesh. In practice, not all volumes get refined simultaneously, so junction dissection schemes are needed, which enlarges the catalogue of shapes, but the latter is bounded nonetheless.)

For these reasons, we shall feel authorized to assume uniformity in this sense. We shall also posit that the hodge entries, whichever way they are built, only depend (up to a multiplicative factor) on the *shapes* of the cells contributing to them. Although stronger than necessary, these assumptions will make some proofs easier, and thus help focus on the main ideas.

4.1 Consistency

Back to the comparison between $\{\mathbf{b}_m, \mathbf{h}_m\}$ and $\{b, h\}$, a natural idea is to compare the computed DoF arrays, $\mathbf{b}_m$ and $\mathbf{h}_m$, with arrays of the same kind, $r_m b = \{\int_f b : f \in \mathcal{F}\}$ and $r_m h = \{\int_{\tilde{f}} h : f \in \mathcal{F}\}$, composed of the fluxes and m.m.f.'s of the (unknown) solution $\{b, h\}$ of the original problem (27). This implicitly defines two operators with the same name, r_m: one that acts on 2-forms, giving an array of facet-fluxes, one that acts on twisted 1-forms, giving an array of dual-edge m.m.f.'s. (No risk of confusion, since the name of the operand, b or h, reveals its nature.)

Since $\mathrm{d}b = 0$, the flux of b embraced by the boundary of any primal 3-cell v must vanish, therefore the sum of facet fluxes $\sum_f \mathbf{D}_{vf} \int_f b$ must vanish for all v. Similarly, $\mathrm{d}h = j$ yields the relation $\sum_f \mathbf{R}^e_f \int_{\tilde{f}} h = \int_{\tilde{e}} j$, by integration over a dual 2-cell. In matrix form, all this becomes

$$\mathbf{D} r_m b = 0, \quad \mathbf{R}^t r_m h = \mathbf{j}, \tag{50}$$

since the entries of $\mathbf{j}$ are precisely the intensities across the dual facets. Comparing with (39), we obtain

$$\mathbf{D}(\mathbf{b}_m - r_m b) = 0, \quad \mathbf{R}^t(\mathbf{h}_m - r_m h) = 0, \tag{51}$$

and

$$(\mathbf{h}_m - r_m h) - \boldsymbol{\nu}(\mathbf{b}_m - r_m b) = (\boldsymbol{\nu} r_m - r_m \nu) b \equiv \boldsymbol{\nu}(r_m \mu - \boldsymbol{\mu} r_m) h. \tag{52}$$

Let us compute the μ-norm of both sides of (52). (For this piece of algebra, we shall use the notation announced in the previous Section: $(\mathbf{b}, \mathbf{h})$ for a sum such as $\sum_{f \in \mathcal{F}} \mathbf{b}_f \mathbf{h}_f$, and $\|\mathbf{h}\|_\mu$ for $(\boldsymbol{\mu}\mathbf{h}, \mathbf{h})^{1/2}$, the μ-norm of $\mathbf{h}$, and other similar constructs.)

As this is done, "square" and "rectangle" terms appear. The rectangle term for the left-hand side is $-2(\mathbf{b}_m - r_m b, \mathbf{h}_m - r_m h)$, but since $\mathbf{D}(\mathbf{b}_m - r_m b) = 0$ implies the existence of some $\mathbf{a}$ such that $\mathbf{b}_m - r_m b = \mathbf{R}\mathbf{a}$, we have

$$(\mathbf{b}_m - r_m b, \mathbf{h}_m - r_m h) = (\mathbf{R}\mathbf{a}, \mathbf{h}_m - r_m h) = (\mathbf{a}, \mathbf{R}^t(\mathbf{h}_m - r_m h)) = 0,$$

after (51). Only square terms remain, and we get

$$\|\mathbf{h}_m - r_m h\|^2_\mu + |\mathbf{b}_m - r_m b|^2_\nu = |(\boldsymbol{\nu} r_m - r_m \nu) b|^2_\mu \equiv |(\boldsymbol{\mu} r_m - r_m \mu) h|^2_\nu \equiv (\boldsymbol{\nu} r_m b - r_m h, r_m b - \boldsymbol{\mu} r_m h). \tag{53}$$

On the left-hand side, which has the dimension of an energy, we spot two plausible estimators for the error incurred by taking $\{\mathbf{b}_m, \mathbf{h}_m\}$ as a substitute for the real field $\{b, h\}$: the "error in (discrete) energy" [resp. coenergy], as regards $\mathbf{b}_m - r_m b$ [resp. $\mathbf{h}_m - r_m h$]. Components of $\mathbf{b}_m - r_m b$ are what can be called the "residual fluxes" $\mathbf{b}_f - \int_f b$, i.e., the difference between the computed flux embraced by facet f and the genuine (but unknown) flux $\int_f b$. Parallel considerations apply to h, with m.m.f.'s along $\tilde{f}$ instead of fluxes. It makes sense to try and *bound* these error terms by some function of γ_m. So let us focus on the right-hand side of (53), for instance on its second expression, the one in terms of h.

By definition of r_m, the f-component of $r_m(\mu h)$ is the flux of $b = \mu h$ embraced by f. On the other hand, the flux array $\boldsymbol{\mu} r_m h$ is the result of applying the discrete Hodge operator to the

m.m.f. array $r_{\mathrm{m}}h$, so the compound operators $r_{\mathrm{m}}\mu$ and $\boldsymbol{\mu} r_{\mathrm{m}}$ will not be equal: they give different fluxes when applied to a generic h. This contrasts with the equalities $(\mathbf{D}r_{\mathrm{m}} - r_{\mathrm{m}}\mathrm{d})b = 0$ and $(\mathbf{R}^t r_{\mathrm{m}} - r_{\mathrm{m}}\mathrm{d})h = 0$, which stem from the Stokes theorem. The mathematical word to express such equalities is "conjugacy": $\mathbf{D}$ and d are conjugate via r_{m}, and so are $\mathbf{R}^t$ and d, too. Thus, μ and $\boldsymbol{\mu}$ are *not* conjugate via r_{m}—and this is, of course, the reason why discretizing entails some error.

Yet, it may happen that $r_{\mathrm{m}}\mu$ and $\boldsymbol{\mu} r_{\mathrm{m}}$ *do* coincide for *some* hs. This is so, for instance, with piecewise constant fields, when $\boldsymbol{\mu}$ is the diagonal hodge of (33) and (34): actually, these formulas were motivated by the desire to achieve this coincidence for such fields. Also, as we shall prove later, $r_{\mathrm{m}}\nu$ and $\boldsymbol{\nu} r_{\mathrm{m}}$ coincide on facet-element approximations of b, i.e., on divergence-free fields of the form $\Sigma_{f\in\mathcal{F}}\mathbf{b}_f w^f$ (which are meshwise constant), when $\boldsymbol{\nu}$ is the Galerkin hodge. Since all piecewise smooth fields differ from such special fields by some small residual, and the finer the mesh the smaller, we may in such cases expect "asymptotic conjugacy", in the sense that the right-hand side of (53) will tend to 0 with m, for a piecewise smooth b or h. This property, which we rewrite informally but suggestively as

$$\boldsymbol{\nu} r_{\mathrm{m}} - r_{\mathrm{m}}\nu \to 0 \text{ when } \mathrm{m} \to 0, \quad \boldsymbol{\mu} r_{\mathrm{m}} - r_{\mathrm{m}}\mu \to 0 \text{ when } \mathrm{m} \to 0 \tag{54}$$

(two equivalent statements), is called *consistency* of the approximation of μ and ν by $\boldsymbol{\mu}$ and $\boldsymbol{\nu}$. Consistency, thus, implies asymptotic vanishing of the error in (discrete) energy, after (53).

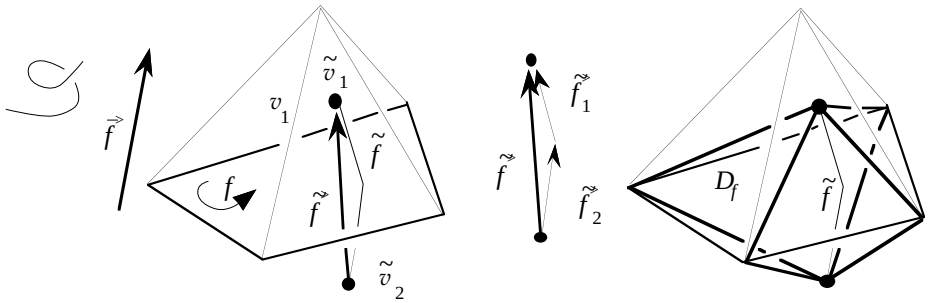

Figure 31. As in Fig. 27, $\vec{f}$ denotes the vectorial area of facet f: the vector of magnitude area(f), normal to f, that points away from f in the direction derived from f's inner orientation by Ampère's rule. By $\tilde{\vec{f}}$ we denote the vector that joins the end points of the associated dual edge $\tilde{f}$. (An ambient orientation is assumed here. One could do without it by treating both $\vec{f}$ and $\tilde{\vec{f}}$ as axial vectors.) In case ν is not the same on both sides of f, understand $\nu\tilde{\vec{f}}$ as $\nu_2\tilde{\vec{f}}_2 + \nu_1\tilde{\vec{f}}_1$, where $\tilde{\vec{f}}_2$ and $\tilde{\vec{f}}_1$ are as suggested. Region D_f is the volume enclosed by the "tent" determined by the extremities of $\tilde{f}$ and the boundary of f. Note that $\vec{f}$ and $\nu\tilde{\vec{f}}$ always cross f in the same direction, but only in the orthogonal construction are they parallel (cf. Fig. 27): In that case, (55) can be satisfied by a *diagonal* hodge—cf. (33) and (34).

Let's now take a heuristic step. (We revert to vector proxies for this. Figure 31 explains about $\vec{f}$ and $\tilde{\vec{f}}$, and n and τ are normal and tangent unit vector fields, as earlier. The norm of an ordinary vector is $|\ |$.) Remark that the right-hand side of (53) is, according to its rightmost avatar, a sum of terms, one for each f, of the form

$$[\Sigma_{f'}\boldsymbol{\nu}^{ff'}\int_{f'} n\cdot\mathrm{B} - \int_{\tilde{f}}\nu\,\tau\cdot\mathrm{B}][\int_f \mu\, n\cdot\mathrm{H} - \Sigma_{f''}\boldsymbol{\mu}^{ff''}\int_{\tilde{f}''}\tau\cdot\mathrm{H}],$$

which we'll abbreviate as $[\mathrm{B}, f][\mathrm{H}, f]$. Each should be made as small as possible for the sum to tend to 0. Suppose ν is uniform, and that boundary conditions are such that B and H are uniform. Then $[\mathrm{B}, f] = \mathrm{B}\cdot(\Sigma_{f'}\boldsymbol{\nu}^{ff'}\vec{f}' - \nu\tilde{\vec{f}})$. This term vanishes if

$$\Sigma_{f'\in\mathcal{F}}\boldsymbol{\nu}^{ff'}\vec{f}' = \nu\tilde{\vec{f}}. \tag{55}$$

(This implies $\Sigma_{f'\in\mathcal{F}}\boldsymbol{\mu}^{ff'}\nu\tilde{\vec{f}}' = \vec{f}$, and hence, cancellation of $[\mathrm{H}, f]$, too.) We therefore adopt this geometric compatibility condition as a *criterion* about $\boldsymbol{\nu}$. Clearly, the diagonal hodge of (34) passes this test. But on the other hand, no diagonal $\boldsymbol{\nu}$ can satisfy (55) unless $\vec{f}$ and $\nu\tilde{\vec{f}}$ are collinear.

Proposition 5. *If $\boldsymbol{\nu}$ is diagonal, with $\boldsymbol{\nu}^{ff}\vec{f} = \nu\vec{\tilde{f}}$, as required by the criterion, there is consistency.*

Proof. (All C's, from now on, denote constants, not necessarily the same each time, possibly depending on the solution, but not on the mesh.) This time, the solution proxy B is only piecewise smooth, and possibly discontinuous if ν is not uniform, but its component parallel to $\vec{f}$, say $\mathcal{B}$, satisfies $|\mathcal{B}(x) - \mathcal{B}(y)| \leq C|x - y|$ in the region D_f of Fig. 31. One has[47] $\int_f n \cdot \mathrm{B} = \mathrm{area}(f)\mathcal{B}(x_f)$ and $\int_{\tilde{f}} \nu\tau \cdot \mathrm{B} = \mathrm{length}(\nu\vec{\tilde{f}})\mathcal{B}(x_{\tilde{f}})$, for some averaging points x_f and $x_{\tilde{f}}$, the distance of which doesn't exceed γ_m, hence $[\mathrm{B}, f] \leq C\gamma_\mathrm{m}\boldsymbol{\nu}^{ff}\mathrm{area}(f)$, by factoring out $\boldsymbol{\nu}^{ff}\mathrm{area}(f) \equiv \mathrm{length}(\nu\vec{\tilde{f}})$, and similarly, $[\mathrm{H}, f] \leq C\gamma_\mathrm{m}\boldsymbol{\mu}^{ff}\mathrm{length}(\nu\vec{\tilde{f}})$. Noticing that $\mathrm{area}(f)\,\mathrm{length}(\nu\vec{\tilde{f}}) = 3\int_{D_f}\nu$, and summing up with respect to f, one finds that

$$\|\mathbf{h}_\mathrm{m} - r_\mathrm{m}h\|_\mu^2 + \|\mathbf{b}_\mathrm{m} - r_\mathrm{m}b\|_\nu^2 \leq C\gamma_\mathrm{m}^2, \tag{56}$$

the consistency result. ◊

Going back to (53), we conclude that both the ν-norm of the residual flux array and the μ-norm of the residual m.m.f. array tend to 0 as fast as γ_m, or faster,[48] a result we shall exploit next.

One may wonder whether the proof can be carried out in the case of a non-diagonal hodge, assuming (55). The author has not been able to do so on the basis of (55) only. The result is true under stronger hypotheses (stronger than necessary, perhaps): When the construction of $\boldsymbol{\nu}$ is a local one, i.e., $\boldsymbol{\nu}^{ff'} = 0$ unless facets f and f' belong to a common volume, and when the *infimum* δ_m of all cell diameters verifies $\delta_\mathrm{m} \geq \beta\gamma_\mathrm{m}$, with β independent of m. Then $\boldsymbol{\nu}$ has a band structure, and its terms behave in γ_m^{-1}, which makes it easy to prove that $[\mathrm{B}, f]$ is in $O(\gamma_\mathrm{m}^2)$. Handling $[\mathrm{H}, f]$ is more difficult, because $\boldsymbol{\mu}$ is full, and the key argument about averaging points not being farther apart than γ_m breaks down. On the other hand, owing to the band structure of $\boldsymbol{\nu}$, and its positive-definite character, $\boldsymbol{\mu}^{ff'}$ is small for distant f and f', which allows one to also bound $[\mathrm{H}, f]$ by $C\gamma_\mathrm{m}^2$. The number of faces being in γ_m^{-3}, consistency ensues.

There is some way to go from such an argument to a proof, but this is enough to confirm (55) in its status of criterion as regards $\boldsymbol{\nu}$, a criterion which is satisfied, by construction (Fig. 27), in FIT [104] and in the cell method [99], but allows a much larger choice. We'll see in a moment how and why it is satisfied in the Galerkin approach.

4.2 Stability

So, the left-hand side of (53) tends to 0. Although this is considered by many as sufficient in practice, one cannot be satisfied with such "discrete energy" estimates. Fields should be compared with fields. To really prove convergence, one should build from the DoF arrays $\mathbf{b}_\mathrm{m}$ and $\mathbf{h}_\mathrm{m}$ an approximation $\{b_\mathrm{m}, h_\mathrm{m}\}$ of the pair of differential forms $\{b, h\}$, and show that the discrepancies $b_\mathrm{m} - b$ and $h_\mathrm{m} - h$ tend to 0 with m in some definite sense. So we are after some map, that we shall denote by p_m, that would transform a flux array $\mathbf{b}$ into a 2-form $p_\mathrm{m}\mathbf{b}$ and an m.m.f. array $\mathbf{h}$ into a twisted 1-form $p_\mathrm{m}\mathbf{h}$. The map should behave naturally with respect to r_m, i.e.,

$$r_\mathrm{m}p_\mathrm{m}\mathbf{b} = \mathbf{b}, \quad r_\mathrm{m}p_\mathrm{m}\mathbf{h} = \mathbf{h}, \tag{57}$$

[47] In case ν is not the same on both sides of f, understand $\mathrm{length}(\nu\vec{\tilde{f}})$ as $\nu_1\mathrm{length}(\vec{\tilde{f}}_1) + \nu_2\mathrm{length}(\vec{\tilde{f}}_2)$. The underlying measure of lengths is not the Euclidean one, but the one associated with the metric induced by the Hodge operator ν.

[48] Convergence in γ_m^2 is in fact often observed when the meshes have some regularity, such as crystal-like symmetries, which may cancel out some terms in the Taylor expansions implicit in the above proof. For instance, the distance between points x_f and $x_{f'}$ may well be in γ_m^2 rather than γ_m. This kind of phenomenon is commonplace in Numerical Analysis [86].

as well as

$$|p_{\mathfrak{m}} r_{\mathfrak{m}} b - b|_\nu \to 0 \text{ and } |p_{\mathfrak{m}} r_{\mathfrak{m}} h - h|_\mu \to 0 \text{ when } \mathfrak{m} \to 0 \tag{58}$$

(asymptotic vanishing of the "truncation error" $p_{\mathfrak{m}} r_{\mathfrak{m}} - 1$). A satisfactory result, then, would be that both $|b - p_{\mathfrak{m}} \mathbf{b}_{\mathfrak{m}}|_\nu$ and $|h - p_{\mathfrak{m}} \mathbf{h}_{\mathfrak{m}}|_\mu$ tend to 0 with $\mathfrak{m}$ (convergence "in energy"). As will now be proved, this is warranted by the following inequalities:

$$\alpha |p_{\mathfrak{m}} \mathbf{b}|_\nu \le |\mathbf{b}|_\nu, \quad \alpha |p_{\mathfrak{m}} \mathbf{h}|_\mu \le |\mathbf{h}|_\mu \tag{59}$$

for all $\mathbf{b}$ and $\mathbf{h}$, where the constant $\alpha > 0$ does not depend on $\mathfrak{m}$. Since $|\mathbf{b}|_\nu$ and $|\mathbf{h}|_\mu$ depend on the discrete hodge, (59) is a property of the approximation scheme, called *stability*.

Proposition 6. *Consistency* (54) *being assumed,* (58) *and* (59) *entail convergence.*

Proof. By consistency, the right-hand side of (53) tends to 0, whence $|\mathbf{b}_{\mathfrak{m}} - r_{\mathfrak{m}} b|_\nu \to 0$, and $|p_{\mathfrak{m}} \mathbf{b}_{\mathfrak{m}} - p_{\mathfrak{m}} r_{\mathfrak{m}} b|_\nu \to 0$ by (59). Therefore $p_{\mathfrak{m}} \mathbf{b}_{\mathfrak{m}} \to b$, "in energy", thanks to (58). Same argument about h. ◊

This is Lax's celebrated folk theorem: *consistency + stability = convergence.*

Below, we shall find a systematic way to construct $p_{\mathfrak{m}}$, the so-called *Whitney map*. But if we don't insist right now on generality, there is an easy way to find a suitable such map in the case of a simplicial primal mesh and of DoF arrays $\mathbf{b}$ that satisfy $\mathbf{D}\mathbf{b} = 0$ (luckily, only these do matter in magnetostatics). The idea is to find a vector proxy $\overline{\mathrm{B}}$ uniform inside each tetrahedron with facet fluxes $\overline{\mathrm{B}} \cdot \vec{f}$ equal to $\mathbf{b}_f$. (Then, $\operatorname{div} \overline{\mathrm{B}} = 0$ all over D.) This, which would not be possible with cells of arbitrary shapes, can be done with tetrahedra, for there are, for each tetrahedral volume v, three unknowns (the components of $\overline{\mathrm{B}}$) to be determined from four fluxes linked by one linear relation, $\sum_f \mathbf{D}_v^f \mathbf{b}_f = 0$, so the problem has a solution, which we take as $p_{\mathfrak{m}} \mathbf{b}$.

Then,[49] $p_{\mathfrak{m}} r_{\mathfrak{m}} b \to b$. As for the stability condition (59), one has $|p_{\mathfrak{m}} \mathbf{b}|_\nu^2 = \int_D \nu |\overline{\mathrm{B}}|^2$, a quadratic form with respect to the facet fluxes, which we may therefore denote by $(\mathbf{b}, \mathbf{N}\mathbf{b})$, with $\mathbf{N}$ some square regular matrix. Now, suppose first a *single* tetrahedron in the mesh $\mathfrak{m}$, and consider the Rayleigh-like quotient $(\mathbf{b}, \boldsymbol{\nu}\mathbf{b})/(\mathbf{b}, \mathbf{N}\mathbf{b})$. Its lower bound, strictly positive, depends only on the *shape* of the tetrahedron, not on its size. Then, uniformity of the family of meshes, and of the construction of $\boldsymbol{\nu}$, allows us to take for α in (59) the smallest of these lower bounds, which is strictly positive and independent of $\mathfrak{m}$. We may thereby conclude that $p_{\mathfrak{m}} \mathbf{b}_{\mathfrak{m}}$ converges towards b in energy.

No similar construction on the side of h is available, but this is not such a handicap: if $p_{\mathfrak{m}} \mathbf{b}_{\mathfrak{m}} \to b$, then $\nu p_{\mathfrak{m}} \mathbf{b}_{\mathfrak{m}} \to h$. This amounts to setting $p_{\mathfrak{m}}$ on the dual side equal to $\nu p_{\mathfrak{m}} \boldsymbol{\mu}$. The problem with that is, $p_{\mathfrak{m}} \mathbf{h}$ fails to have the continuity properties we expect from a magnetic field: its vector proxy H is not tangentially continuous across facets, so one cannot take its curl. But never mind, since this "non-conformal" approximation converges in energy.

Yet, we need a more encompassing $p_{\mathfrak{m}}$ map, if only because $\mathbf{D}\mathbf{b} = 0$ was just a happy accident. Before turning to that, which will be laborious, let's briefly discuss convergence in the full Maxwell case.

4.3 The time-dependent case

Here is a sketch of the convergence proof for the generalized Yee scheme (36)(37) of last Section.

[49] This is an exercise, for which the following hints should suffice. Start from b, piecewise smooth, such that $\mathrm{d}b = 0$, set $\mathbf{b} = r_{\mathfrak{m}} b$, get $\overline{\mathrm{B}}$ as above, and aim at finding an upper bound for $|\mathrm{B} - \overline{\mathrm{B}}|$, where B is the proxy of b, over a tetrahedron T. For this, evaluate $\nabla\lambda \cdot \int_{\mathrm{T}} (\mathrm{B} - \overline{\mathrm{B}})$, where λ is an affine function such that $|\nabla\lambda| = 1$. Integrate by parts, remark that $\int_f \lambda\, n \cdot \overline{\mathrm{B}} = \lambda(x_f) \mathbf{b}_f$, where x_f is the barycenter of f. Taylor-expand $n \cdot \mathrm{B}$ about x_f, hence a bound in $C\gamma_{\mathfrak{m}}^4$ for $\int_{\partial \mathrm{T}} \lambda\, n \cdot (\mathrm{B} - \overline{\mathrm{B}})$, from which stems $|\int_{\mathrm{T}} (\mathrm{B} - \overline{\mathrm{B}})| \le C\gamma_{\mathfrak{m}}^4$. Use uniformity to conclude that $|\mathrm{B} - \overline{\mathrm{B}}| \le C\gamma_{\mathfrak{m}}$.

First, linear interpolation in time between the values of the DoF arrays, as output by the scheme, provides DoF-array-valued functions of time which converge, when δt tends to zero, towards the solution of the "spatially discretized" equations (31)(32). This is not difficult.

Next, linearity of the equations allows one to pass from the time domain to the frequency domain, via a Laplace transformation. Instead of studying (31)(32), therefore, one may examine the behavior of the solution of

$$-p\,\mathbf{D} + \mathbf{R}^t\mathbf{H} = \mathbf{J}, \quad p\,\mathbf{B} + \mathbf{R}\mathbf{E} = 0, \tag{60}$$

$$\mathbf{D} = \boldsymbol{\epsilon}\,\mathbf{E}, \quad \mathbf{B} = \boldsymbol{\mu}\mathbf{H}, \tag{61}$$

when $\mathrm{m} \to 0$. Here, $p = \xi + \mathrm{i}\omega$, with $\xi > 0$, and small capitals denote Laplace transforms, which are arrays of *complex*-valued DoFs. If one can prove uniform convergence with respect to ω (which the requirement $\xi > 0$ makes possible), convergence of the solution of (31)(32) will ensue, by inverse Laplace transformation. The main problem, therefore, is to compare $\mathbf{E}$, $\mathbf{B}$, $\mathbf{H}$, $\mathbf{D}$, as given by (60)(61), with $r_{\mathrm{m}}\mathrm{E}, r_{\mathrm{m}}\mathrm{B}, r_{\mathrm{m}}\mathrm{H}, r_{\mathrm{m}}\mathrm{D}$, where small capitals, again, denote Laplace transforms, but of differential forms this time.

The approach is similar to what we did in statics. First establish that

$$p\boldsymbol{\mu}(\mathbf{H} - r_{\mathrm{m}}\mathrm{H}) + \mathbf{R}(\mathbf{E} - r_{\mathrm{m}}\mathrm{E}) = p(r_{\mathrm{m}}\mu - \boldsymbol{\mu} r_{\mathrm{m}})\mathrm{H}, \tag{62}$$

$$-p\boldsymbol{\epsilon}\,(\mathbf{E} - r_{\mathrm{m}}\mathrm{E}) + \mathbf{R}^t(\mathbf{H} - r_{\mathrm{m}}\mathrm{H}) = -p(r_{\mathrm{m}}\epsilon - \boldsymbol{\epsilon}\, r_{\mathrm{m}})\mathrm{E}. \tag{63}$$

Then, right-multiply (62) (in the sense of $(\ ,\ )$) by $(\mathbf{H} - r_{\mathrm{m}}\mathrm{H})^*$ and the complex conjugate of (63) by $-(\mathbf{E} - r_{\mathrm{m}}\mathrm{E})$, add. The middle terms (in $\mathbf{R}$ and $\mathbf{R}^t$) cancel out, and energy estimates follow. The similarity between the right-hand sides of (52), on the one hand, and (62)(63), on the other hand, shows that no further consistency requirements emerge. Stability, thanks to $\xi > 0$, holds there if it held in statics. What is a good discrete hodge in statics, therefore, is a good one in transient situations. Let's tentatively promote this remark to the rank of heuristic principle:

As regards discrete constitutive laws, *what makes a convergent scheme for* static *problems will, as a rule, make one for the Maxwell evolution equations as well.*

At this stage, we may feel more confident about the quality of the toolkit: If the discrete hodges and the meshes are compatible in the sense of (55), so that consistency can be achieved, if there is a way to pass from DoFs to fields which binds energy and discrete energy tightly enough for stability (59) to hold, then convergence will ensue. So we need the p_{m} operator. We would need it, anyway, to determine fluxes, emf's, etc., at a finer scale than what the mesh provides—motivation enough to search for interpolants, but not the most compelling reason to do so: Field reconstruction from the DoFs is needed, basically, *to assess stability,* in the above sense, and thereby, the validity of the method. Whitney forms, which will now enter the scene, provide this mechanism.

4.4 Whitney forms

Let's summarize the requirements about the generic map p_{m}. It should map each kind of DoF array to a differential form of the appropriate kind: $p_{\mathrm{m}}\mathbf{e}$, starting from an edge-based DoF array $\mathbf{e}$, should be a 1-form; $p_{\mathrm{m}}\mathbf{b}$, obtained from a facet-based $\mathbf{b}$, should be a 2-form, and so forth. Properties (57) and (58) should hold for all kinds, too, so in short,

$$r_{\mathrm{m}}p_{\mathrm{m}} = 1, \quad p_{\mathrm{m}}r_{\mathrm{m}} \to 1 \quad \text{when} \quad \mathrm{m} \to 0. \tag{64}$$

The stability property (59) will automatically be satisfied in the case of a uniform family of meshes. Moreover, we expect $\mathrm{d}b = 0$ when $\mathbf{D}\mathbf{b} = 0$, $\mathrm{d}e = 0$ when $\mathbf{R}\mathbf{e} = 0$, etc. More generally, $\mathbf{R}\mathbf{a} = \mathbf{b}$ should entail $\mathrm{d}a = b$, and so forth. These are desirable features of the toolkit. The neatest way to secure them is to enforce the structural property

$$\mathrm{d}p_{\mathrm{m}} = p_{\mathrm{m}}\mathbf{d}, \tag{65}$$

at all levels (Fig. 32): d and **d** should be conjugate, via p_m, or said differently, Fig. 32 should be a *commutative diagram*. Remarkably, these prescriptions will prove sufficient to generate interpolants in an essentially unique way. Such interpolants are known as *Whitney forms* [109], and we shall refer to the structure they constitute as the *Whitney complex*.

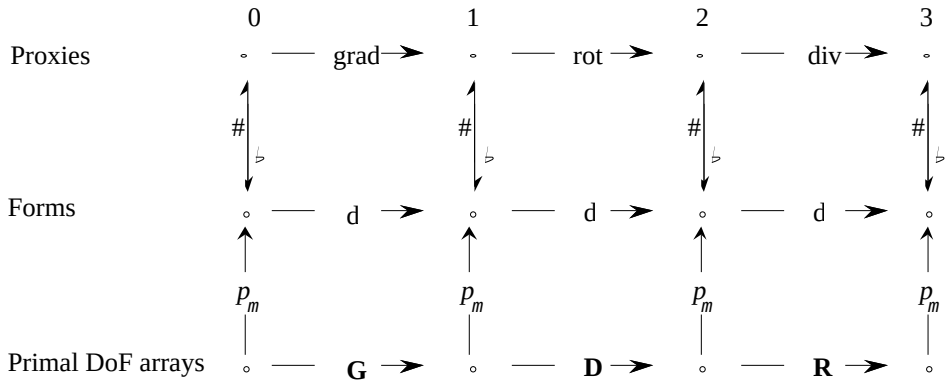

Figure 32. Diagrammatic rendering of (65), with part of Fig. 13 added. Flat and sharp symbols represent the isomorphism between differential forms and their scalar or vector proxies.

4.4.1 Whitney forms as a device to approximate manifolds

We address the question by taking a detour, to see things from a viewpoint consistent with our earlier definition of differential forms as maps from manifolds to numbers. A differential form, say, for definiteness, b, maps a p-manifold S to the number $\int_S b$, with $p = 2$ here. Suppose we are able to approximate S by a p-chain, i.e., here, a chain based on facets, $p^i_m S = \sum_{f \in \mathcal{F}} \mathbf{c}^f f$. Then a natural approximation to $\int_S b$ is $\int_{p^i_m S} b$. But this number we know, by linearity: since $\int_f r_m b = \mathbf{b}_f$, it equals the sum $\sum_f \mathbf{c}^f \mathbf{b}_f$, that we shall denote $\langle \mathbf{c} \,;\, \mathbf{b} \rangle$ (with boldface brackets). Hence an approximate knowledge of the field b, i.e., of all its measurable attributes—the fluxes—from the DoF array $\mathbf{b}$. In particular, fluxes embraced by *small* surfaces (with respect to the grain of the mesh) will be computable from $\mathbf{b}$, which meets our expectations about interpolating to local values of b. The question has thus become "how best to represent S by a 2-chain?". Figure 33 (where $p = 1$, so a curve c replaces S) gives the idea.

Once we know about the manifold-to-chain map p^i_m, we know about Whitney forms: For instance, the one associated with facet f is, like the field b itself, a map from surfaces to numbers, namely the map $S \to \mathbf{c}^f$ that assigns to S its weight with respect to f. We denote this map by w^f and its value at S by $\int_S w^f$ or by $\langle S \,;\, w^f \rangle$ as we have done earlier. (The notational redundancy will prove useful.) Note that $\langle\!\langle p^i_m S \,;\, \mathbf{b} \rangle\!\rangle = \int_S \sum_f \mathbf{b}_f w^f = \int_S p_m \mathbf{b} \equiv \langle S \,;\, p_m \mathbf{b} \rangle$, which justifies the "$p^i_m$" notation: A transposition is indeed involved.

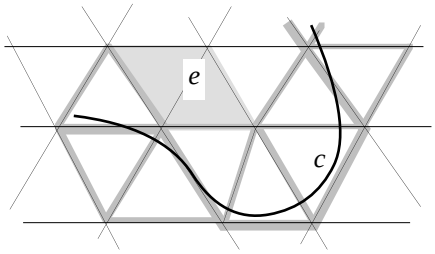

Figure 33. Representing curve c by a weighted sum of mesh-edges, i.e., by a 1-chain. Graded thicknesses of the edges are meant to suggest the respective weights assigned to them. Edges such as e, whose "control domain" (shaded) doesn't intersect c, have zero weight. (A weight can be negative, if the edge is oriented backwards with respect to c.) Which weights thus to assign is the central issue in our approach to Whitney forms.

4.4.2 A generating formula

Now, let's enter the hard core of it. A simplicial primal mesh will be assumed until further notice. (We shall see later how to lift this restriction.) Results will hold for any spatial dimension n and all simplicial dimensions $p \leq n$, but will be stated as if n was 3 and $p = 1$ or 2 (edge and facet elements). So we shall also write proofs, even recursive ones that are supposed to move from p to $p+1$ (see, e.g., Prop. 7), as if p had a specific value (1 or 2), and thereby prefer $\mathbf{R}, \mathbf{D}$, or $\mathbf{R}^t, \mathbf{D}^t$, to $\mathbf{d}$ or $\boldsymbol{\partial}$. That the proof has general validity notwithstanding should be obvious each time.

We use $\lambda^n(x)$ for the barycentric weight of point x with respect to node n, when x belongs to one of the tetrahedra which share node n (otherwise, $\lambda^n(x) = 0$). We'll soon see that $w^n = \lambda^n$ is the natural choice for nodal 0-forms, and again this dual notation will make some formulas more readable. We define $\lambda^e = \lambda^m + \lambda^n$, when edge $e = \{m, n\}$, as well as $\lambda^f = \lambda^l + \lambda^m + \lambda^n$ for facet $f = \{l, m, n\}$, etc. When $e = \{m, n\}$ and $f = \{l, m, n\}$, we denote node l by $f - e$. Thus λ^{f-e} refers to (in that case) λ^l, and equals $\lambda^f - \lambda^e$. The oriented segment from point x to point y is xy, the oriented triangle formed by points x, y, z, in this order, is xyz. And although node n and its location x_n should not be confused, we shall indulge in writing, for instance, ijx for the triangle based on points x_i, x_j, and x, when i and j are node labels.

The weights in the case of a "small manifold", such as a point, a segment, etc.,[50] will now be constructed, and what to use for non-small ones, i.e., the maps w^e, w^f, etc., from lines, surfaces, etc., to reals, will follow by linearity. The principle of this construction is to enforce the following commutative diagram property:

$$\boldsymbol{\partial}\, p^t_{\mathrm{m}} = p^t_{\mathrm{m}} \partial, \tag{66}$$

which implies, by transposition, $\mathrm{d} p_{\mathrm{m}} = p_{\mathrm{m}} \mathbf{d}$, the required structural property (65).[51] We shall not endeavor to prove, step by step, that our construction does satisfy (66), although that would be an option. Rather, we shall let (66) inspire the definition that follows, and then, directly establish that $\mathrm{d} p_{\mathrm{m}} = p_{\mathrm{m}} \mathbf{d}$. This in turn will give (66) by transposition.

Definition. *Starting from $w^n = \lambda^n$, the simplicial Whitney forms are*

$$w^e = \sum_{n \in \mathcal{N}} \mathbf{G}^n_e \, \lambda^{e-n} \mathrm{d} w^n, \; w^f = \sum_{e \in \mathcal{E}} \mathbf{R}^e_f \, \lambda^{f-e} \mathrm{d} w^e, \; w^v = \sum_{f \in \mathcal{F}} \mathbf{D}^f_v \, \lambda^{v-f} \mathrm{d} w^f \tag{67}$$

(and so on, recursively, to higher dimensions).

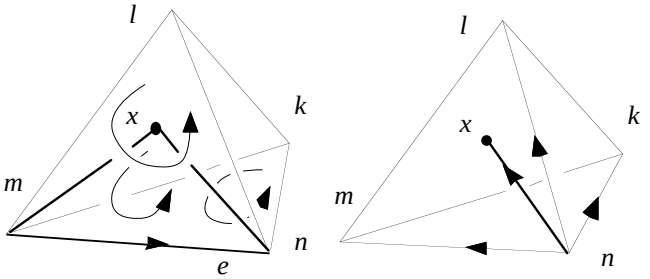

Figure 34. Left: With edge $e = \{m, n\}$ and facets $\{m, n, k\}$ and $\{m, n, l\}$ oriented as shown, the 2-chain to associate with the "join" $x \vee e$, alias mnx, can only be $\lambda^k(x)\, mnk + \lambda^l(x)\, mnl$. This is what (68) says. Right: Same relation between the join $x \vee n$ and the 1-chain $\lambda^k(x)\, nk + \lambda^l(x)\, nl + \lambda^m(x)\, nm$.

Let us justify this statement, by showing how compliance with (66) suggests these formulas. The starting point comes from finite element interpolation theory, which in our present stand

[50] The proper underlying concept, not used here, is that of *multivector* at point x.

[51] If moreover $\ker(\boldsymbol{\partial}_p) = \mathrm{cod}(\boldsymbol{\partial}_{p+1})$, i.e., in the case of a trivial topology, $\ker(\mathrm{d}_p) = \mathrm{cod}(\mathrm{d}_{p-1})$, just as, by transposition, $\ker(\mathbf{d}_p) = \mathrm{cod}(\mathbf{d}_{p-1})$. One says the Whitney spaces of forms, as linked by the d_p, form an *exact sequence*.

consists in expressing a point x as a weighted sum of nodes, the weights $w^n(x)$ being the barycentric ones, $\lambda^n(x)$. (Note how the standard p_{m} for nodal DoFs, $p_{\mathrm{m}}\varphi = \sum_n \varphi_n w^n$, comes from $p^t_{\mathrm{m}} x = \sum_n w^n(x)\, n$ by transposition.) Recursively, suppose we know the proper weights for a segment yz, i.e., the bracketed terms in the sum $p^t_{\mathrm{m}} yz = \sum_e \langle yz\,;\, w^e\rangle\, e$, and let us try to find $p^t_{\mathrm{m}} xyz$. By linearity, $p^t_{\mathrm{m}} xyz = \sum_e \langle yz\,;\, w^e\rangle\, p^t_{\mathrm{m}}(x \vee e)$, where the "join" $x \vee e$ is the triangle displayed in Fig. 34, left. So the question is: which 2-chain best represents $x \vee e$? As suggested by Fig. 34, the only answer consistent with (66) is

$$p^t_{\mathrm{m}}(x \vee e) = \sum_{f \in \mathcal{F}} \mathbf{R}^e_f\, \lambda^{f-e}(x)\, f. \tag{68}$$

Indeed, this formula expresses $x \vee e$ as the average of mnk and mnl (the only two facets f for which $\mathbf{R}^e_f \neq 0$), with weights that depend on the relative proximity of x. So $p^t_{\mathrm{m}} xyz = \sum_{e,f} \mathbf{R}^e_f\, \lambda^{f-e}(x)\, \langle yz\,;\, w^e\rangle f \equiv \sum_f \langle xyz\,;\, w^f\rangle\, f$, hence

$$\langle xyz\,;\, w^f\rangle = \sum_e \mathbf{R}^e_f\, \lambda^{f-e}(x)\, \langle yz\,;\, w^e\rangle. \tag{69}$$

On the other hand, since a degenerate triangle such as xzx should get zero weights, we expect $0 = \langle xzx\,;\, w^f\rangle = \sum_e \mathbf{R}^e_f \lambda^{f-e}(x) \langle zx\,;\, w^e\rangle$, and the same for $\langle xxy\,;\, w^f\rangle$. From this (which will come out true after Prop. 7 below), we get

$$\langle xyz\,;\, w^f\rangle = \sum_e \mathbf{R}^e_f\, \lambda^{f-e}(x)\, \langle yz + zx + xy\,;\, w^e\rangle$$

$$= \sum_e \mathbf{R}^e_f\, \lambda^{f-e}(x)\, \langle \partial(xyz)\,;\, w^e\rangle = \sum_e \mathbf{R}^e_f\, \lambda^{f-e}(x)\, \langle xyz\,;\, \mathrm{d}w^e\rangle$$

for any small triangle xyz, by Stokes, and hence $w^f = \sum_e \mathbf{R}^e_f\, \lambda^{f-e}\, \mathrm{d}w^e$.

Thus, formulas (67)—which one should conceive as the unfolding of a unique formula—are forced on us, as soon as we accept (68) as the right way, amply suggested by Fig. 34, to pass from the weights for a simplex s to those for the join $x \vee s$. The reader will easily check that (67) describes the Whitney forms as they are more widely known, that is, on a tetrahedron $\{k, l, m, n\}$,

$$w^n = \lambda^n$$

for node n,

$$w^e = \lambda^m \mathrm{d}\lambda^n - \lambda^n \mathrm{d}\lambda^m$$

for edge $e = \{m, n\}$,

$$w^f = 2(\lambda^l \mathrm{d}\lambda^m \wedge \mathrm{d}\lambda^n + \lambda^m \mathrm{d}\lambda^n \wedge \mathrm{d}\lambda^l + \lambda^n \mathrm{d}\lambda^l \wedge \mathrm{d}\lambda^m)$$

for facet $f = \{l, m, n\}$, and

$$w^v = 6(\lambda^k \mathrm{d}\lambda^l \wedge \mathrm{d}\lambda^m \wedge \mathrm{d}\lambda^n + \lambda^l \mathrm{d}\lambda^m \wedge \mathrm{d}\lambda^n \wedge \mathrm{d}\lambda^k + \lambda^m \mathrm{d}\lambda^n \wedge \mathrm{d}\lambda^k \wedge \mathrm{d}\lambda^l + \lambda^n \mathrm{d}\lambda^k \wedge \mathrm{d}\lambda^l \wedge \mathrm{d}\lambda^m)$$

for volume $v = \{k, l, m, n\}$. In higher dimensions [109], the Whitney form of a p-simplex $s = \{n_0, n_1, \ldots, n_p\}$, with inner orientation implied by the order of the nodes, is

$$w^s = p! \sum_{i=0,\ldots p} (-1)^i\, w^{n_i} \mathrm{d}w^{n_0} \wedge \ldots \langle i \rangle \ldots \wedge \mathrm{d}w^{n_p},$$

where the $\langle i \rangle$ means "omit the term $\mathrm{d}w^{n_i}$".

From now on, we denote by W^p the finite-dimensional subspaces of $\mathcal{F}^p$ generated by these basic forms.

Remark. To find the vector proxies of w^e and w^f, substitute ∇ and $\times$ to d and $\wedge$. The scalar proxy of w^v is simply the function equal to $1/\operatorname{vol}(v)$ on v, 0 elsewhere. The reader is invited to establish the following formulas:

$$w^{mn}(x) = (kl \times kx)/6 \operatorname{vol}(klmn), \quad w^{mnk}(x) = xl/3 \operatorname{vol}(v),$$

very useful when it comes to actual coding. (Other handy formulas, at this stage, are $\mathrm{rot}(x \to v \times ox) = 2v$ and $\mathrm{div}(x \to ox) = 3$, where o is some origin point and v a fixed vector. As an exercise, one may use this to check on Prop. 9 below.) $\diamondsuit$

Remark. One may recognize in (69) the development of the 3×3 determinant of the array of barycentric coordinates of points x, y, z, with respect to nodes l, m, n, hence the geometrical interpretation of the weights displayed in Fig. 35. $\diamondsuit$

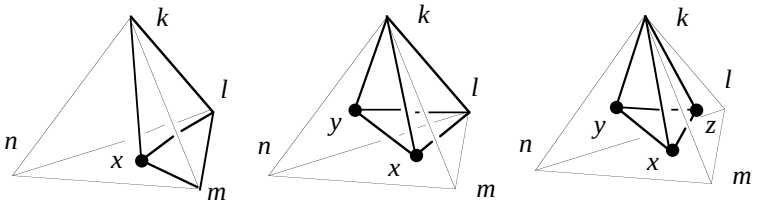

Figure 35. Just as the barycentric weight of point x with respect to node n is $\mathrm{vol}(klmx)$, if one takes $\mathrm{vol}(klmn)$ as unity, the weight of the segment xy with respect to edge $\{m, n\}$ is $\mathrm{vol}(klxy)$, and the weight of the triangle xyz with respect to facet $\{l, m, n\}$ is $\mathrm{vol}(kxyz)$.

4.4.3 Properties of Whitney forms

Thus in possession of a rationale for (67), we now derive from it a few formulas, for their own sake and as a preparation for the proof of the all important $\mathrm{d}p_{\mathrm{m}} = p_{\mathrm{m}}\mathbf{d}$ result, Prop. 9 below.

Proposition 7. *For each p-simplex, there is one linear relation between Whitney forms associated with $(p-1)$-faces of this simplex. For instance, for each f,*

$$\sum_{e \in \mathcal{E}} \mathbf{R}^e_f \, \lambda^{f-e} \, w^e = 0.$$

Proof: By (67), $\sum_e \mathbf{R}^e_f \, \lambda^{f-e} \, w^e = \sum_{e,n} \lambda^{f-e} \lambda^{e-n} \mathbf{R}^e_f \mathbf{G}^n_e \, w^n = 0$, thanks to the relation $\mathbf{RG} = 0$, because $\lambda^{f-e}\lambda^{e-n}$, which is the same for all e in ∂f, can be factored out. $\diamondsuit$

As a corollary, and by using $\mathrm{d}(\lambda\omega) = \mathrm{d}\lambda \wedge \omega + \lambda \, \mathrm{d}\omega$, we have

$$w^f = -\sum_{e \in \mathcal{E}} \mathbf{R}^e_f \, \mathrm{d}\lambda^{f-e} \wedge w^e,$$

and other similar alternatives to (67).

Proposition 8. *For each p-simplex s, one has*

$$\text{(70)} \qquad \text{(i)} \;\; \lambda^s \mathrm{d}w^s = (p+1)\, \mathrm{d}\lambda^s \wedge w^s, \quad \text{(ii)} \;\; \mathrm{d}\lambda^s \wedge \mathrm{d}w^s = 0.$$

Proof. This is true for $p = 0$. Assume it for $p = 1$. Then $\mathrm{d}w^f = \sum_e \mathbf{R}^e_f \, \mathrm{d}\lambda^{f-e} \wedge \mathrm{d}w^e = \sum_e \mathbf{R}^e_f \, \mathrm{d}\lambda^f \wedge \mathrm{d}w^e \equiv \mathrm{d}\lambda^f \wedge \sum_e \mathbf{R}^e_f \, \mathrm{d}w^e$ by (70*ii*), hence $\mathrm{d}\lambda^f \wedge \mathrm{d}w^f = 0$. Next, $\lambda^f \mathrm{d}w^f = \lambda^f (\sum_e \mathbf{R}^e_f \, \mathrm{d}\lambda^f \wedge \mathrm{d}w^e) = \mathrm{d}\lambda^f \wedge (\sum_e \mathbf{R}^e_f \lambda^f \mathrm{d}w^e) = \mathrm{d}\lambda^f \wedge (w^f + \sum_e \mathbf{R}^e_f \lambda^e \mathrm{d}w^e)$, which thanks to (70*i*) equals $\mathrm{d}\lambda^f \wedge (w^f + 2\sum_e \mathbf{R}^e_f \, \mathrm{d}\lambda^e \wedge w^e) = \mathrm{d}\lambda^f \wedge w^f - 2\, \mathrm{d}\lambda^f \wedge \sum_e \mathbf{R}^e_f \, \mathrm{d}\lambda^{f-e} \wedge w^e = 3\, \mathrm{d}\lambda^f \wedge w^f$, which proves (70*i*) for $p = 2$. Hence (70*ii*) for $p = 2$ by taking the d. $\diamondsuit$

Next, yet another variant of (67), but without summation this time. For any edge e such that $\mathbf{R}^e_f \neq 0$, one has

$$\text{(71)} \qquad \mathbf{R}^e_f w^f = \lambda^{f-e} \mathrm{d}w^e - 2\, \mathrm{d}\lambda^{f-e} \wedge w^e.$$

This is proved by recursion, using $\mathbf{G}^n_{e'} w^{e'} = \lambda^{e'-n} \mathrm{d}w^n - \mathrm{d}\lambda^{e'-n} w^n$, where $n = e \cap e'$, and the identity $\mathbf{G}^n_{e'} \mathbf{G}^n_e = -\mathbf{R}^{e'}_f \mathbf{R}^e_f$. We may now conclude with the main result about structural properties (cf. Fig. 32):

Proposition 9. *One has*

$$\mathrm{d}w^e = \sum_{f \in \mathcal{F}} \mathbf{R}^e_f w^f,$$

and hence, by linearity, $\mathrm{d}p_{\mathfrak{m}} = p_{\mathfrak{m}}\mathbf{d}$.

Proof. Since both sides vanish out of the "star" of e, i.e., the union $\mathrm{st}(e)$ of volumes containing it, one may do as if $\mathrm{st}(e)$ was the whole meshed region. Note that $\sum_f \mathbf{R}^e_f \lambda^f = 1 - \lambda^e$ on $\mathrm{st}(e)$. Then, $\sum_f \mathbf{R}^e_f w^f = \sum_f [\lambda^{f-e}\mathrm{d}w^e - 2\,\mathrm{d}\lambda^{f-e} \wedge w^e] = (1-\lambda^e)\mathrm{d}w^e - 2\,\mathrm{d}(1-\lambda^e) \wedge w^e = (1-\lambda^e)\mathrm{d}w^e + \lambda^e \wedge \mathrm{d}w^e \equiv \mathrm{d}w^e$, by using (70*i*). Now, $\mathrm{d}(p_{\mathfrak{m}}\mathbf{a}) = \mathrm{d}(\sum_e \mathbf{a}_e w^e) = \sum_{e,f} \mathbf{R}^e_f \mathbf{a}_e w^f = \sum_f (\mathbf{R}\mathbf{a})_f w^f = p_{\mathfrak{m}}(\mathbf{d}\mathbf{a})$. ◊

As a corollary, $\mathrm{d}W^{p-1} \subset W^p$, and if $\ker(\mathbf{d}_p) = \mathrm{cod}(\mathbf{d}_{p-1})$, then $\ker(\mathrm{d}\,; W^p) = \mathrm{d}\,W^{p-1}$, the *exact sequence* property of Whitney spaces in case of trivial topology.

4.4.4 "Partition of unity"

For what comes now, we revert to the standard vector analysis framework, where w^f denotes the proxy vector field (i.e., $2(\lambda^l \nabla\lambda^m \times \nabla\lambda^n + \ldots)$) of the Whitney form w^f.

Recall that barycentric functions sum to 1, thus forming a "partition of unity": $\sum_{n\in\mathcal{N}} w^n = 1$. We shall drop the ugly arrows in what follows, and use symbol f not only as a label, but also for the vectorial area of f (Fig. 31). Same dual use of $\tilde{f}$. Same convention for xyz, to be understood as a triangle or as its vectorial area, according to the context.

Proposition 10. *At all points* x*, for all vectors* v*,*

$$\sum_{f\in\mathcal{F}} (w^f(x)\cdot v)\, f = v. \tag{72}$$

This is a case of something true of all simplices, and a consequence of the above construction in which the weights $\langle xyz\,; w^f(x)\rangle$ were assigned in order to have $xyz = \sum_f \langle xyz\,; w^f(x)\rangle f$. Replacing there w^f by its proxy, and xyz and f by their vectorial areas, we find (72). As a corollary (replace f by g, v by $\nu w^f(x)$, and integrate in x), the entries $\boldsymbol{\nu}^{fg}$ of the Galerkin facet elements mass matrix satisfy

$$\sum_{g\in\mathcal{F}} \boldsymbol{\nu}^{fg} g = \nu\tilde{f}$$

where $\nu\tilde{f}$ is as explained on Fig. 31, but with the important specification that here, we are dealing with the *barycentric* dual mesh. That $\int \nu w^f = \nu\tilde{f}$ is an exercise in elementary geometry, and a similar formula holds for all Whitney forms (Fig. 36). Now, compare this with (55), the compatibility condition that was brought to light by the convergence analysis: We have proved, at last, that the Galerkin hodges do satisfy it.

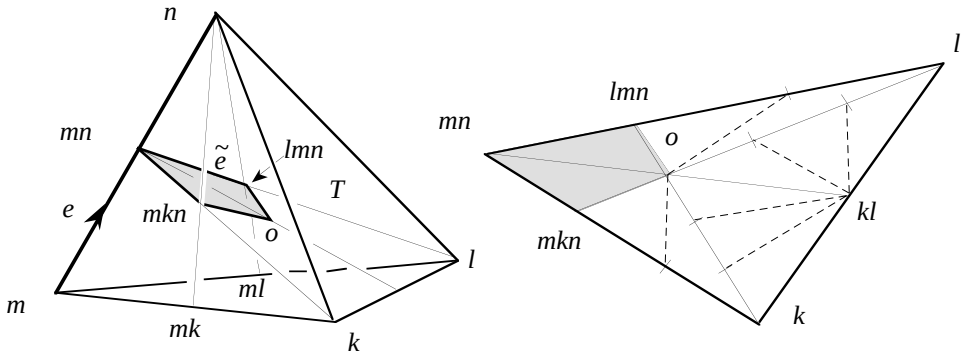

Figure 36. Why $\int_{\mathrm{T}} w^e = \check{e}$ in the barycentric construction of the dual mesh. First, the length of the altitude from n is $1/|\nabla w^n|$, therefore $\int_T \nabla w^n = klm/3$. Next, the average of w^n or w^m is $1/4$. So $\int_{\mathrm{T}} w^e \equiv \int_{\mathrm{T}} [w^m \nabla w^n - w^n \nabla w^m]$ is a vector equal to $(klm/3 + kln/3)/4$. As the figure shows (all twelve triangles on the right have the same area), this is precisely the vectorial area of $\check{e}$.

5. Higher-degree forms

Let's sum up: Whitney forms were built in such a way that the partition of unity property (72) ensues. This property makes the mass matrix $\boldsymbol{\nu}$ of facet elements satisfy, with respect to the

mesh and its barycentric dual, a compatibility criterion, (55), which we earlier recognized as a requisite for consistency. Therefore, we may assert that *Whitney forms of higher polynomial degree,* too, *should satisfy* (72), and take this as heuristic guide in the derivation of such forms.

Being a priori more numerous, higher-degree forms will make a finer partition. But we have a way to refine the partition (72): Multiply it by the λ^ns, which themselves form a partition of unity. This results in

$$\sum_{f\in\mathcal{F},n\in\mathcal{N}} (\lambda^n w^f(x)\cdot v)\, f = v,$$

hence the recipe: Attach to edges, faces, etc., the products $\lambda^n w^e$, $\lambda^n w^f$, etc., where n spans $\mathcal{N}$. Instead of the usual Whitney spaces W^p, with forms of polynomial degree 1 at most, we thus obtain larger spaces W_2^p, with forms of polynomial degree 2 at most. (For consistency, W^p may now be denoted W_1^p.) As we shall prove in a moment (under the assumption of trivial topology, but this is no serious restriction), the complex they constitute enjoys the exact sequence property : If for instance $b = \sum_{n,f} \mathbf{b}_{nf}\lambda^n w^f$ satisfies $\mathrm{d}b = 0$ (which means it has a divergence-free proxy) then there are DoFs $\mathbf{a}_{ne}$ such that $b = \mathrm{d}(\sum_{n,e} \mathbf{a}_{ne}\lambda^n w^e)$. (How to define W_k^p, for polynomial degrees $k = 3, \ldots$, should now be obvious.)

Note however that, because of Prop. 7, these new forms are not linearly independent. For instance, the span of the $\lambda^n w^e$s, over a tetrahedron, has dimension 20 instead of the apparent 24, because Prop. 7 imposes one linear relation per facet. Over the whole mesh, with N nodes, E edges, F facets, the two products $\lambda^m w^e$ and $\lambda^n w^e$ for each edge $e = \{m, n\}$, and the three products $\lambda^{f-e} w^e$ for each facet f, make a total of $2E + 3F$ generators for W_2^1. But with one relation per facet, the dimension of W_2^1 is only $2(E + F)$. (The spans of the $\lambda^n w^n$s, the $\lambda^n w^f$s, and the $\lambda^n w^v$s, have respective dimensions $N + E$, $3(F + V)$, and $4V$. The general formula is $\dim(W_2^p) = (p + 1)(S_p + S_{p+1})$, where S_p is the number of p-simplices. Note that $\sum_p (-1)^p \dim(W_2^p) = \sum_p (-1)^p S_p \equiv \chi$, the Euler–Poincaré constant of the meshed domain.)

Owing to this redundancy, the main problem with these forms is, how to interpret the DoFs. With standard edge elements, the DoF $\mathbf{a}_{e'}$ is the integral of the 1-form $a = \sum_e \mathbf{a}_e w^e$ over edge e'. In different words, the square matrix of the circulations $\langle e' \,;\, w^e \rangle$ is the unit matrix: edges and edge elements are *in duality* in this precise sense (just like the basis vectors and covectors ∂_i and d^j of Note 26). Here, we cannot expect to find a family of 1-chains in such duality with the $\lambda^n w^e$s. The most likely candidates in this respect, the "small edges" denoted $\{n, e\}$, etc., on Fig. 37, left, don't pass, because the matrix of the $\langle \{n', e'\} \,;\, \lambda^n w^e \rangle$ is not the unit matrix. If at least this matrix was regular, finding chains in duality with the basis forms, or the other way round, would be straightforward. But regular it is not, because of the relations of Prop. 7. We might just omit one small edge out of three on each face, but this is an ugly solution. Better to reason in terms of *blocks* of DoF of various dimensions, and to be content with a rearragement of chains that makes the matrix block-diagonal: Blocks of size 1 for small edges which are part of the "large" ones, blocks of size three for small edges inside the facets. Each of these 3-blocks corresponds to a subspace of dimension *two*, owing to Prop. 7, be it the subspace of forms or of chains. The triple of degrees of freedom, therefore, is up to an additive constant. Yet, the circulations[52] do determine the *form*, if not the DoF, uniquely ("unisolvence" property).

[52] Since the matrix has no maximal rank, small-edge circulations must satisfy compatibility conditions for the form to exist. (Indeed, one will easily check that any element of W_2^1 has a null circulation along the chain made by the boundary of a facet minus four times the boundary of the small facet inside it.) This raises a minor problem with the r_{m} map, whose images need not satisfy this condition. The problem is avoided with a slightly different definition of the small edges [57], as suggested on the right of Fig. 37.

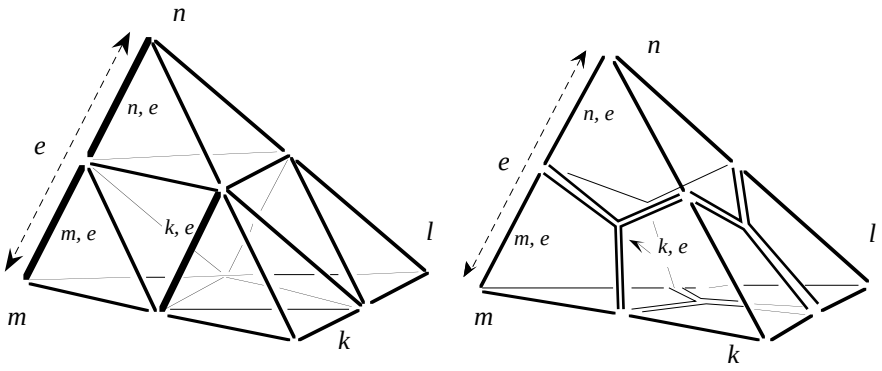

Figure 37. Left: "Small" edges, in one-to-one correspondence with the forms $\lambda^n w^e$, and how they are labelled. Right: A variant where some small edges, such as $\{k, e\}$, are broken lines. These three crooked small edges, with proper signs, add up to the null chain, hence the compatibility condition of Note 52 is built in.

The reader will easily guess about "small facets" (16 of them on a single tetrahedron, for a space of dimension $3(F+T) = 3(4+1) = 15$) and "small volumes" (four), in both variants.

Which leaves us with the task of proving the exact sequence property, that is to say, the validity of Poincaré's Lemma in the complex of the W_2^p: Show that $\mathrm{d}b = 0$ for $b \in W_2^p$ implies the existence, locally at least, of $a \in W_2^{p-1}$ such that $b = \mathrm{d}a$. We'll treat the very case this notation suggests, i.e., $p = 2$, and assume trivial topology ("contractible" meshed domain), which does no harm since only a local result is aimed at. We use rot and div rather than d for more clarity. First, two technical points:

Lemma 1: *If* $\sum_{n\in\mathcal{N}} \beta_n \lambda^n(x) = \beta_0$ *for all* x, where the βs are real numbers, *then* $\beta_n = \beta_0$ *for all nodes* $n \in \mathcal{N}$.

Proof. Clear, since $\sum_n \lambda^n = 1$ is the only relation linking the $\lambda^n(x)$s. ♢

Lemma 2: *If* $a \in W^1$, *then* $2\,\mathrm{rot}(\lambda^n a) - 3\,\lambda^n\,\mathrm{rot}\,a \in W^2$.

Proof. If $a = w^e$ and $n = f - e$, this results from (71). If n is one of the end points of e, e.g., $e = \{m, n\}$, a direct computation, inelegant as it may be, will do: $2\,\mathrm{d}\lambda^n \wedge (\lambda^m \mathrm{d}\lambda^n - \lambda^n \mathrm{d}\lambda^m) = -2\,\lambda^n \mathrm{d}\lambda^n \wedge \mathrm{d}\lambda^m = \lambda^n \mathrm{d}w^e$. ♢

Now,

Proposition 11. *If the* W_1^p *sequence is exact, the* W_2^p *sequence is exact.*

Proof (at level $p = 2$). Suppose $b = b_0 + \sum_{n\in\mathcal{N}} \lambda^n b_n$, with b_0 and all the b_n in W^2, and $\mathrm{div}\,b = 0$. Taking the divergence of the sum and applying Lemma 1 in each volume, one sees that $\mathrm{div}\,b_n$ is the same field for all n. So there is some common $\bar{b}$ in W^2 such that $\mathrm{div}(b_n - \bar{b}) = 0$ for all n, and since the W^p complex is exact, there is an a_n in W^1 such that $b_n = \bar{b} + \mathrm{rot}\,a_n$. Hence, $b = b_0 + \bar{b} + \sum_n \lambda^n\,\mathrm{rot}\,a_n$. By Lemma 2, there is therefore some $\hat{b}$ in W^2 such that $b = \hat{b} + \frac{2}{3}\,\mathrm{rot}(\sum_n \lambda^n a_n)$. Since $\mathrm{div}\,\hat{b} = 0$, the solenoidal b in W_2^2 we started from is indeed the curl of some element of W_2^1. ♢

Very little is needed to phrase the proof in such a way that the contractibility assumption becomes moot. Actually, the complexes W_1^p and W_2^p have *the same cohomology*, whatever the topology of the domain and the culling of passive simplices (i.e., those bearing a null DoF) implied by the boundary conditions.

4.6 Whitney forms for other shapes than simplices

This simple idea, *approximate p-manifolds by p-chains based on p-cells of the mesh*, is highly productive, as we presently see.

4.6.1 Hexahedra

First example, the well-known isoparametric element [39] on hexahedra can thus be un-

derstood. A 2D explanation (Fig. 38) will suffice, the generalization being easy. Let us take a convex quadrangle based on points $x_{00}, x_{10}, x_{01}, x_{11}$, and wonder about which weights $w^n(x)$ should be assigned to them (label n designates the generic node) in order to have $x = \sum_{n\in\{00,10,10,11\}} w^n(x)\, x_n$ in a sensible way. The weights are obvious if x lies on the boundary. For instance, if $x = (1-\xi)x_{00} + \xi x_{10}$, a point we shall denote by $x_{\xi 0}$, weights are $\{1-\xi, \xi, 0, 0\}$. Would it be $x \equiv x_{\xi 1} = (1-\xi)x_{01} + \xi x_{11}$, we would take $\{0, 0, 1-\xi, \xi\}$. Now, each x is part of some segment $[x_{\xi 0} x_{\xi 1}]$, for a *unique* value $\xi(x)$ of the weight ξ, in which case $x = (1-\eta)x_{\xi 0} + \eta x_{\xi 1}$, for some $\eta = \eta(x)$, hence it seems natural to distribute the previous weights in the same proportion:

$$(73)\quad x = (1-\eta(x))(1-\xi(x))\, x_{00} + (1-\eta(x))\xi(x)\, x_{10} + \eta(x)(1-\xi(x))\, x_{01} + \eta(x)\xi(x)\, x_{11},$$

and we are staring at the basis functions. They form, obviously, a partition of unity.

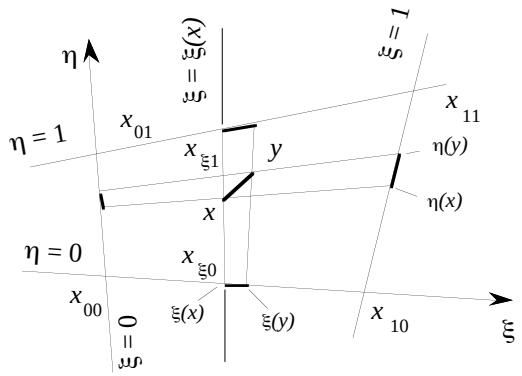

Figure 38. The system of projections, in dimension 2.

Looking at what we have done, and generalizing to dimension 3 or higher, we notice a *system of projections,* associated with a trilinear[53] *chart*, $x \to \{\xi(x), \eta(x), \zeta(x)\}$, from a hexahedron to the unit cube in $\xi\eta\zeta$-space. The successive projections (which can be performed in any order) map a point $x \equiv x_{\xi\eta\zeta}$ to its images $x_{0\eta\zeta}$ and $x_{1\eta\zeta}$ on opposite facets[54] $\xi = 0$ and $\xi = 1$, then, recursively, send these images to points on opposite edges, etc., until eventually a node n is reached. In the process, the weight $\langle x\,;\, w^n\rangle$ of x is recursively determined by formulas such as (assuming for the sake of the example that n belongs to the facet $\xi = 0$)

$$\langle x_{\xi\eta\zeta}\,;\, w^n\rangle = (1-\xi)\langle x_{0\eta\zeta}\,;\, w^n\rangle.$$

The final weight of x with respect to n is thus the product of factors, such as here $(1-\xi)$, collected during the projection process. (They measure the relative proximity of each projection to the face towards which next projection will be done.) The last factor in this product is 1, obtained when the projection reaches n. Observe the fact, essential of course, that whatever the sequence of projections, the partial weights encountered along the way are the same, only differently ordered, and hence the weight of x with respect to node n is a well-defined quantity.

The viewpoint thus adopted makes the next move obvious. Now, instead of a point x, we deal with a vector v at x, small enough for the segment xy (where $y = x + v$) to be contained in a single hexahedron. The above projections send x and y to facets, edges, etc. Ending the downward recursion one step higher than previously, at the level of edges, we get projections $x_e y_e$ of xy onto all edges e. The weight $\langle xy\,;\, w^e\rangle$ is the product of weights of x collected along the way, but the last factor is now the algebraic ratio $x_e y_e / e$ (which makes obvious

[53] thus called because ξ, η, and ζ, though cubic polynomials in terms of the Cartesian coordinates of x, are affine functions of each of them, taken separately.

[54] Be aware that p-faces need not be "flat", i.e., lie within an affine p-subspace for $p > 1$, in dimension higher than 2. We assume a mesh generation which avoids this.

sense) instead of 1. Hence the analytical expression of the corresponding Whitney form, for instance, in the case of Fig. 39, $w^e = \eta\zeta \mathrm{d}\xi$. (Notice the built-in "partition of unity" property: $xy = \Sigma_e \langle xy\,;w^e\rangle e$.) The proxies, $w^e = \eta\zeta\nabla\xi$ in this example, were proposed as edge elements for hexahedra in [107].

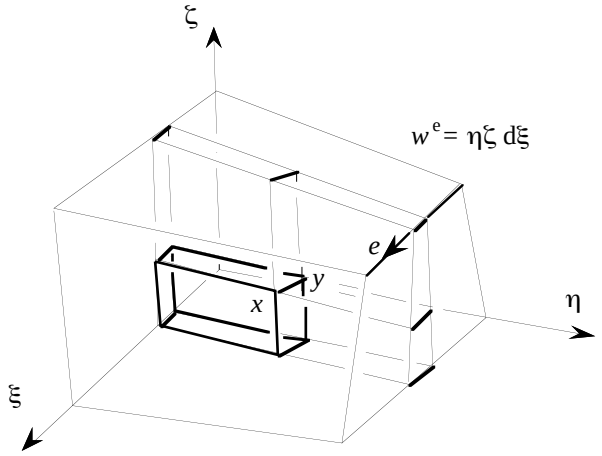

Figure 39. Weight $w^e(xy)$ is the $\xi\eta\zeta$-volume of the "hinder region" of xy with respect to edge e.

One may wonder whether weights such as $\langle xy\,;w^e\rangle$ have a geometric interpretation there too. They have: $\langle xy\,;w^e\rangle$ is the relative volume, in the *reference hexahedron*[55] $H = \{\xi,\eta,\zeta\} : 0 \le \xi \le 1,\ 0 \le \eta \le 1,\ 0 \le \zeta \le 1$, of the "hinder region" of Fig. 39, made of points "behind" xy with respect to edge e. This may seem fairly different from the situation in Fig. 35, middle, but a suitable reinterpretation of the system of projections in the tetrahedron (Fig. 40) shows the analogy.

A similar reasoning gives facet elements: the last weight, for a small triangle xyz, is $x_f y_f z_f / f$, which again makes sense: Take the ratio of the areas (an affine notion) of the images of these surfaces in the reference cube, with sign + if orientations of $x_f y_f z_f$ and f match, − otherwise. Whitney forms such as $w^f = \xi\,\mathrm{d}\eta\,\mathrm{d}\zeta$ (when f is the facet $\xi = 1$) result. The proxy of that particular one is $\xi\,\nabla\eta \times \nabla\zeta$.

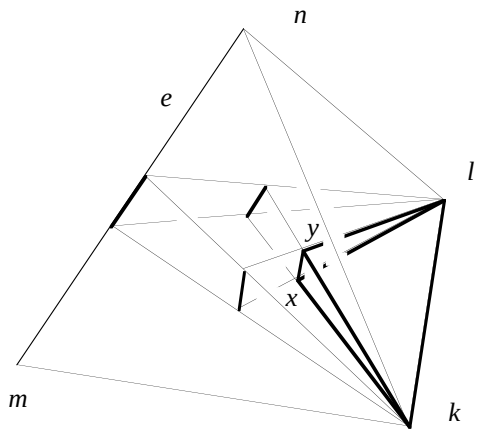

Figure 40. There too, weight $w^e(xy)$ is the relative volume of the hinder region.

4.6.2 Prisms

So, Cartesian coordinates and barycentric coordinates provide two systems of projections which make obvious the weight allocation. These systems can be mixed: one of them in use

[55] Recall that all tetrahedra are affine equivalent, which is why we had no need for a reference one. The situation is different with hexahedra, which form several orbits under the action of the affine group.

for $p < n$ dimensions, the other one for the $n - p$ remaining dimensions. In dimension 3, this gives only one new possibility, the prism (Fig. 41).

Such a variety of shapes makes the mesh generation more flexible [35]. Yet, do the elements of a given degree, edge elements say, fit together properly when one mixes tetrahedra, hexahedra, and prisms? Yes, because of the recursivity of the weight allocation: If a segment xy lies entirely in the facet common to two volumes of different kind, say a tetrahedron and a prism, the weights $\langle xy\,;\, w^e\rangle$ for edges belonging to this facet only depend on what happens in the facet, i.e., they are the same as evaluated with both formulas for w^e, the one valid in the tetrahedron, the one valid in the prism. This is enough to guarantee the *tangential continuity* of such composite edge elements.

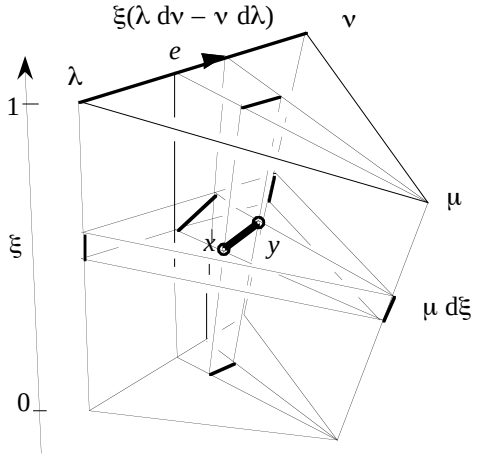

Figure 41. Projective system and edge elements for a prism. Observe the commutativity of the projections

4.6.3 "Degeneracies"

Yet one may yearn for even more flexibility, and edge elements for *pyramids* have been proposed [29, 45]. A systematic way to proceed, in this respect, is to recourse to "degenerate" versions of the hexahedron or the prism, obtained by fusion of one or more pair of nodes and or edges.

To grasp the idea, let's begin with the case of the degenerated quadrilateral, in two dimensions (Fig. 42). With the notations of the Figure, where $\{\lambda, \mu, \nu\}$ are the barycentric coordinates in the left triangle, the map $\{\mu, \nu\} \to \{\eta, \xi\}$, where $\eta = \nu/(\mu + \nu)$ and $\xi = \mu + \nu$, sends the interior of the triangle to the interior of the right quadrilateral. When, by deformation of the latter, x_{10} merges with x_{00}, the projective system of the quadrilateral generates a new projective system on the triangle.

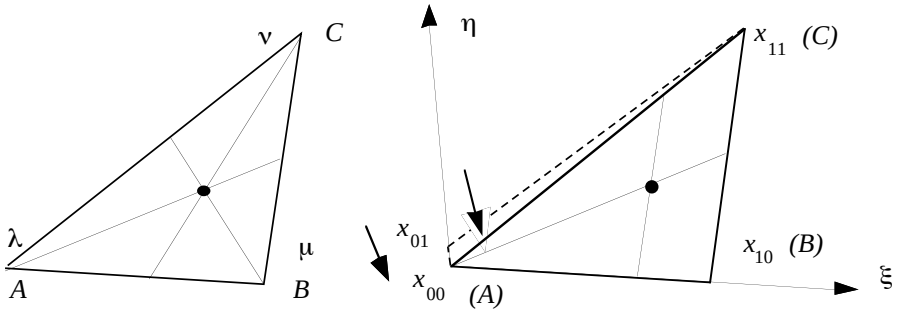

Figure 42. Projective systems for the same triangle, in the barycentric coordinates on the left, and by degeneracy of the quadrilateral system on the right.

The weights assigned to the nodes, and hence the nodal elements, are the same in both systems, for $\xi\eta = \nu$ for point C (cf. (73)), $\xi(1 - \eta) = \mu$ for B, and the sum $(1 - \xi)(1 - \eta)$

$+ (1-\xi)\eta$, attributed to A by adding the loads of x_{00} and x_{01}, does equal λ. But the edge elements differ: For AC, $\eta \mathrm{d}\xi \equiv -(1-\lambda)^{-1}\mu \mathrm{d}\lambda$ on the right instead of $\lambda \mathrm{d}\nu - \nu \mathrm{d}\lambda$ on the left, $-(1-\lambda)^{-1}\mu \mathrm{d}\lambda$ for AB, and $\mathrm{d}\nu + (1-\lambda)^{-1}\nu \mathrm{d}\lambda$ for BC. (The singularity of shape functions at point A is never a problem, because integrals they enter in always converge.)

In dimension 3, the principle is the same: When two edges merge, by degeneration of a hexahedron or of a prism, the Whitney form of the merger is the sum of the Whitney forms of the two contributors, which one may wish to rewrite in a coordinate system adapted to the degenerate solid. Figs 43 and 44 show seven degeneracies, all those that one can obtain from a hexahedron or a prism with plane facets under the constraint of not creating curved facets in the process. As one sees, the only novel shape is the pyramid, while the prism is retrieved once and the tetrahedron four times.

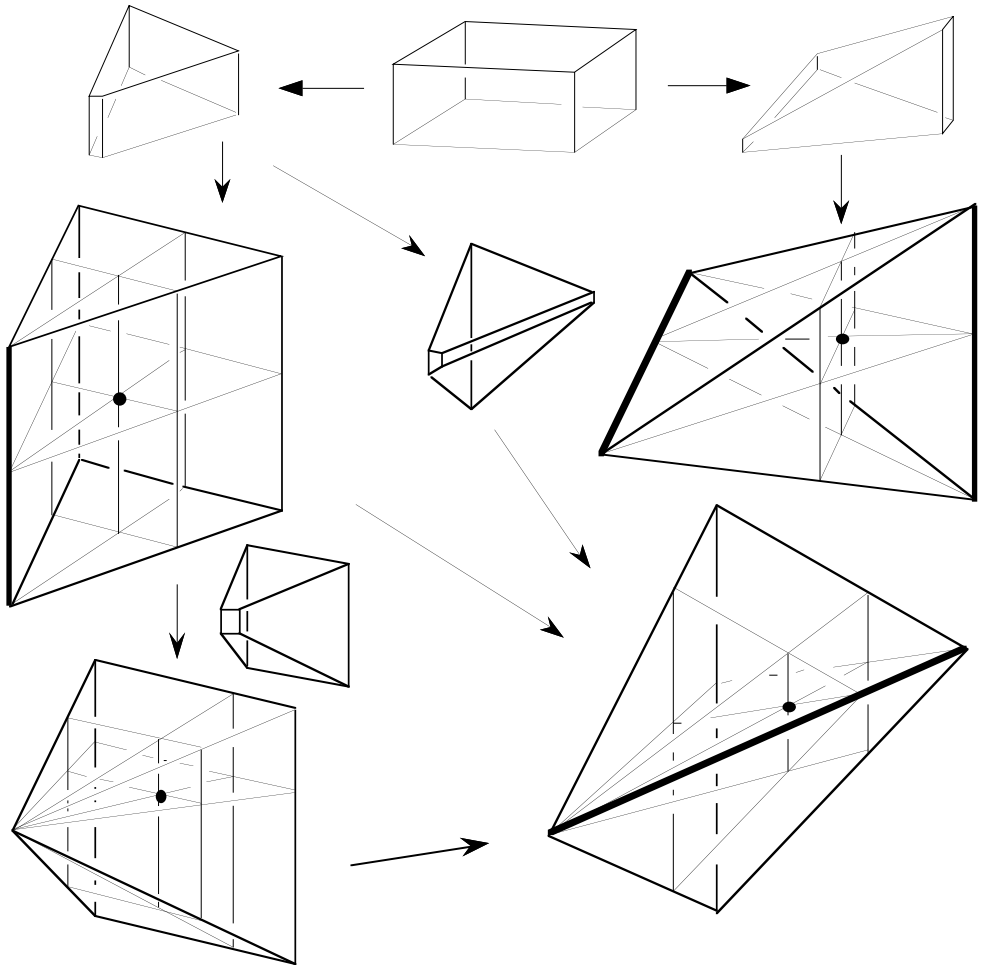

Figure 43. Projective systems in four degenerations of the hexahedron. Thick lines indicate the merged edges.

But, as was predictible from the 2-dimensional case, it's *new* Whitney forms, on these solids, that are produced by the merging, because the projection systems are different. In particular, we have now *five* distinct projective systems on the tetrahedron (and two on the pyramid and the prism), and the equality of traces is not automatic any longer. One must therefore care about correct assembly, in order to get the same projection system on each facet.

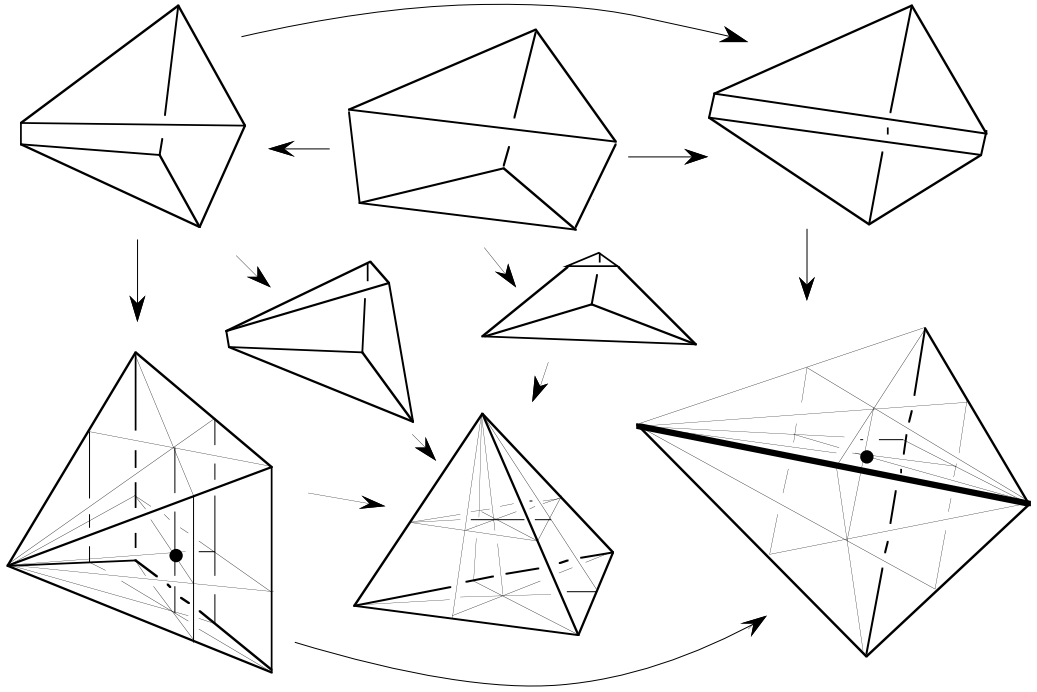

Figure 44. Projective systems in three degenerations of the prism. Note how the pyramid has two ways to degenerate towards the tetrahedron.

The advantage of having the pyramid available is thus marred by the necessity of an extended shape-functions catalogue (on at least two triangular facets of a pyramid, the projection system cannot match the tetrahedron's one), and by the existence of cumbersome assembly rules. Yet, finding the new shape-functions is not too difficult, as exemplified by Figs 45 and 46.

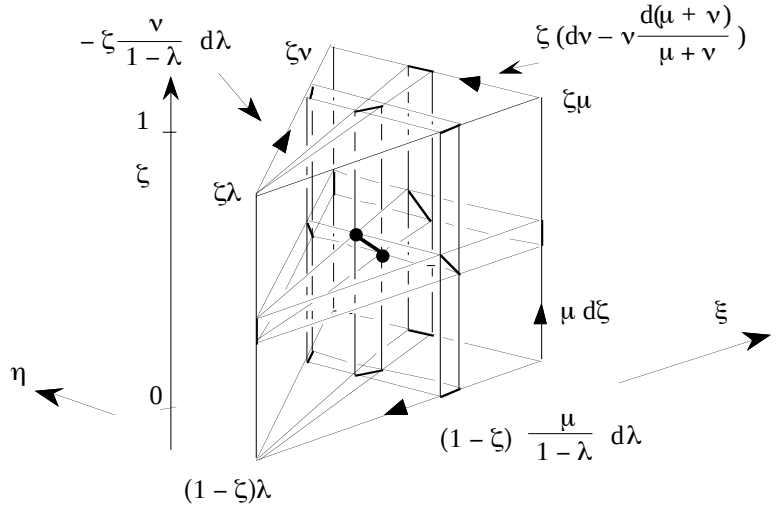

Figure 45. Nodal and edge elements for the projective system of Fig. 43. One passes from the previous coordinate system $\{\xi, \eta, \zeta\}$ to the prism-adapted $\{\zeta, \lambda, \mu, \nu\}$ system by the formulas $\xi = \mu + \nu,\ \eta = \nu/(\mu + \nu)$, with $\lambda + \mu + \nu = 1$.

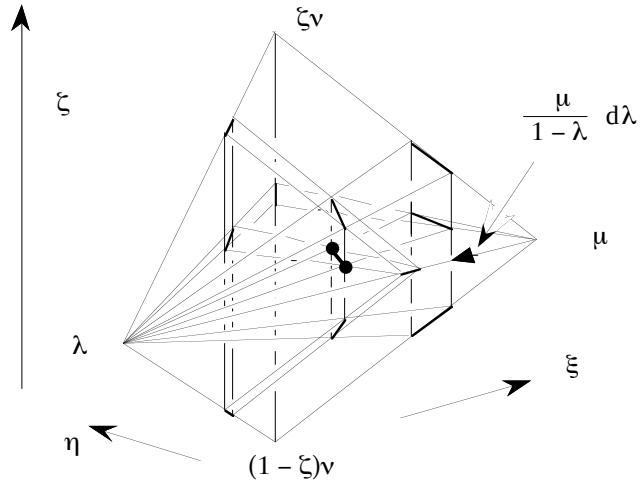

Figure 46. Degeneration of the prism of Fig. 46. Two edges disappear, and a new edge element, $\mu(1-\lambda)^{-1}\mathrm{d}\lambda$ is created by the merging. The coordinate system is the same here as in Fig. 45, so $\{\lambda, \mu, \nu\}$ should not be confused with barycentric coordinates of this tetrahedron. Denoting the latter by $\{\bar\kappa, \bar\lambda, \bar\mu, \bar\nu\}$, and using the formulas $\nu = \bar\nu + \bar\kappa$ and $\zeta = \bar\nu/(\bar\nu + \bar\kappa)$, hence $\xi = \bar\mu + \bar\nu + \bar\kappa = 1 - \bar\lambda$, $\zeta = \bar\nu/(\bar\nu + \bar\kappa)$. Thus, for instance, the shape function $\mu(1-\lambda)^{-1}\mathrm{d}\lambda$ rewrites as $\bar\mu(1-\bar\lambda)^{-1}\mathrm{d}\bar\lambda$ in barycentric coordinates.

4.6.4 Star-shaped cells, dual cells

Let's end all this by an indication on how to build Whitney forms on any star-shaped polyhedron.

Suppose each p-cell of the mesh m, for all p, has been provided with a "center", in the precise sense of §3.3, i.e., a point with respect to which the cell is star-shaped. Then, join the centers in order to obtain a simplicial refinement, $\overline{\mathrm{m}}$ say, where the new sets of p-simplices are $\overline{\mathcal{S}}_p$, the old sets of cells being $\mathcal{S}_p$. In similar style, let $\mathbf{u}$ and $\overline{\mathbf{u}}$ stand for DoF arrays indexed over $\mathcal{S}_p$ and $\overline{\mathcal{S}}_p$ respectively, with the compatibility relation $\mathbf{u}_s = \Sigma_{s'} \pm \overline{\mathbf{u}}_{s'}$ for all s in $\mathcal{S}_p$, the sum running over all small simplices in the refinement of cell s, and the signs taking care of relative orientations. To define $p_{\mathrm{m}}\mathbf{u}$, knowing what $p_{\overline{\mathrm{m}}}\overline{\mathbf{u}}$ is, we just take the *smallest*, in the energy norm, of the $p_{\overline{\mathrm{m}}}\overline{\mathbf{u}}$'s, with respect to all $\overline{\mathbf{u}}$'s compatible with $\mathbf{u}$.

The family of interpolants thus obtained is to the cellular mesh, for all purposes, what Whitney forms were to a simplicial mesh. Whether they deserve to be called "Whitney forms" is debatable, however, because they are metric-dependent, unlike the standard Whitney forms. The same construction on the dual side provides similar pseudo-Whitney forms on the dual mesh. (More precisely, there is, as we have observed at the end of §3.3, a common simplicial refinement of both m and $\widetilde{\mathrm{m}}$. The process just defined constructs forms on both, but it's easy to check that the pseudo-whitneys on the *primal* mesh are just the Whitney forms.) This fills a drawer in the toolkit the emptiness of which we took some pain to hide until now, although it was conspicuous at places, on Fig. 32, for instance.